



**One-step Roll-to-roll Process of Stable AgNW/PEDOT:PSS  
Solution Using Imidazole as Mild Base for Highly Conductive  
and Transparent Films: Optimizations and Mechanisms**

Journal:	<i>Journal of Materials Chemistry C</i>
Manuscript ID:	TC-ART-03-2015-000801.R1
Article Type:	Paper
Date Submitted by the Author:	28-Apr-2015
Complete List of Authors:	Kim, Seyul; Yonsei university, ; Yonsei University, Department of Chemical and Biomolecular Engineering Kim, So Yeon; Yonsei University, Department of Chemical and Biomolecular Engineering Chung, Moon Hyun; Yonsei University, Department of Chemical and Biomolecular Engineering Kim, Jeonghun; University of Wollongong, Institute for Superconducting and Electronic Materials Kim, Jung Hyun; Yonsei University, Department of Chemical and Biomolecular Engineering

## ARTICLE

# One-step Roll-to-roll Process of Stable AgNW/PEDOT:PSS Solution Using Imidazole as Mild Base for Highly Conductive and Transparent Films: Optimizations and Mechanisms

Cite this: DOI: 10.1039/x0xx00000x

Received 00th January 2012,  
Accepted 00th January 2012

DOI: 10.1039/x0xx00000x

[www.rsc.org/](http://www.rsc.org/)

Seyul Kim<sup>a</sup>, So Yeon Kim<sup>a</sup>, Moon Hyun Chung<sup>a</sup>, Jeonghun Kim<sup>b</sup>, and Jung Hyun Kim<sup>a\*</sup>

Recent increase in the demand for transparent electrodes has led to shortage in supply and increase in the price of indium tin oxide (ITO) films deposited by sputter coating owing to coating speed limitations. Furthermore, flexibility has become one of the essential properties of transparent electrodes, accounting for the rapidly changing trend in electronics. These problems can be overcome by AgNW-based films suitable for flexible and stable conductive electrodes by using wet-coating-processable material and roll-to-roll coating. In this work, we developed an effective method to fabricate highly conductive, transparent, and stable AgNW/PEDOT:PSS film using roll-to-roll slot-die coating. This coating technique provides higher line speed and greater coating uniformity. Furthermore, the optimized AgNW/PEDOT:PSS solution allows direct one-step coating without any post-treatment, such as high-temperature annealing, mechanical pressure, and solvent washing. We also studied the mechanisms of AgNW corrosion induced by the acidity of PEDOT:PSS and by hydrogen sulfide (H<sub>2</sub>S) and carbonyl sulfide (OCS) of the atmosphere. Corrosion could be prevented by neutralizing PEDOT:PSS using imidazole, which is a suitable organic compound in terms of both material and processing properties owing to its mild basicity and high melting and boiling points. In addition, the over-coating by silica-based protecting layer on the AgNW/PEDOT:PSS film resulted in enhanced corrosion protection. The resulting roll film (460 mm in width × 20 m in length) showed suitable electrical ( $R_s \sim 75 \Omega \text{ sq}^{-1}$ ) and optical ( $T > 90\%$  at 550 nm, haziness  $\sim 1.21\%$ ,  $b^* \sim 0.72$ ) properties to replace ITO films in touch screen panels.

## Introduction

In the last decade, the trend in electronics is noticeably moving from performance to flexibility, along with remarkable technological progress. Therefore, many research groups attempt to replace the widely used but brittle electrode material indium tin oxide (ITO) to keep pace with the rapid changes in the electronics industry. However, it is not easy to develop alternative materials because of the high transparency and electrical conductivity of ITO compared with other conducting materials, such as carbon nanotubes (CNT), graphene, metallic nanowires, and conducting polymers. Among the conducting materials, metallic nanowires are considered as the best candidate for ITO replacement because only metallic nanowires can be deposited from solution by a coating process and

achieve the performance equivalent to that of ITO. Indeed, metallic nanomaterials, such as silver, copper, and gold have conductivities that are higher than 50 times that of ITO,<sup>1,2</sup> and open holes within the nanowire network dramatically improve the optical transparency.<sup>3</sup> Although metallic nanowires show good electrical and optical properties, they cannot be used directly as transparent electrode for organic photovoltaics (OPV) or organic light-emitting diodes (OLED) because of the large-sized holes and inhomogeneous resistance distribution throughout the conducting film, which gives rise to the degradation of the device performances, resulting from inefficient electron collection.<sup>4</sup> Furthermore, the microscale surface roughness makes it even more inappropriate for application as transparent electrode. To overcome these disadvantages, new methods like the composite approach using

conducting polymers, such as poly(3,4-ethylenedioxythiophene): poly(styrenesulfonate) (PEDOT:PSS) and polyaniline (PANI), while maintaining the advantages of metallic nanowires are researched.<sup>5–10</sup> PEDOT:PSS is the most commonly used composite material owing to its high conductivity and transparency. In addition, incorporating PEDOT:PSS into metallic nanowire networks enhances the electrical properties because it can serve as electrical bridge between individual nanowires. However, high acidity and water absorption of PEDOT:PSS lead to poor stability of the metallic nanowires resulting from acidic corrosion and oxidation induced by excess sulfonic acid groups ( $-\text{SO}_3\text{H}$ ) of PSS, respectively.<sup>11–18</sup> In the case of PANI, although it has higher work function, UV radiation resistance, and chemical stability than PEDOT:PSS, its poor conductivity and the addition of strong acids required for doping cause acidic corrosion and high sheet resistance in conducting films based on metal nanowire.

Recently, Chen et al. reported on the multi-step production of AgNW/PEDOT:PSS hybrid film under ambient air condition by using neutralized PEDOT:PSS as overcoat layer.<sup>9</sup> This pH-neutral PEDOT:PSS was prepared by adding guanidine, which is a strong base with relatively low melting and boiling point. Unfortunately, the conductivity of neutralized PEDOT:PSS was greatly reduced by about 60% and further coating processes of PEDOT:PSS could not help to fabricate a smooth surface on top of the AgNW network exhibiting a surface roughness at the microscale, which is strongly related to the resistance and quality of the resulting transparent electrode. In addition, additive binders were required for the preparation of the AgNW dispersion to prevent AgNW aggregation during the film deposition on the substrate. However, those insulating binders can disturb the electron transfer from PEDOT:PSS to AgNW because almost all of the binders are attached to the nanowire surface. Therefore, this multi-step method cannot maximize the electron transfer through PEDOT:PSS in the AgNW networks. Typically, AgNW-based conducting films undergo some post-treatment, such as high-temperature annealing, mechanical pressure, and solvent washing-off.<sup>19–21</sup> However, those post-treatments eventually generate increased manufacturing costs. In addition, the prepared AgNW/PEDOT:PSS conductive film should undergo rigorous dry and wet processing at high temperature and high humidity during film formation and device fabrication using a roll-to-roll system. Therefore, further developments including the two aspects of materials and processing are needed to achieve superior AgNW/PEDOT:PSS films with low resistance, high transparency, and good stability that can be used as transparent electrodes in future devices.

In this study, AgNW/PEDOT:PSS films were fabricated by direct one-step coating without any post-treatment. The optimized film showed the sheet resistance of  $10.8 \Omega \text{ sq}^{-1}$  and transmittance of 92% at 550 nm. Furthermore, a highly smooth surface was obtained as a result of the almost complete incorporation of AgNWs in PEDOT:PSS. The corrosion of AgNWs caused by the acidity of PEDOT:PSS was carefully analyzed under various conditions, such as room temperature,

high temperature (85 °C), and high temperature and high humidity (85 °C / 85%) using two types of PEDOT:PSS. The pH values of PEDOT:PSS were confirmed by adjusting the amount of added base material, and neutralized PEDOT:PSS can be obtained without serious conductivity loss as a result of optimization of the base materials. Finally, we demonstrate the fabrication of highly transparent, conductive, and stable AgNW/PEDOT:PSS roll film with large area (460 mm in width  $\times$  20 m in length) using roll-to-roll slot-die coating.

## Experimental

### Preparation of AgNW/PEDOT:PSS hybrid ink

The silver nanowire (AgNW) solution was obtained from Nanopyxis in form of a dispersion in deionized water (DI water). The supplied AgNW solution was further diluted in DI water without further purification to prepare the AgNW solution with the concentration of  $5 \text{ mg mL}^{-1}$ . Then, the diluted solution was stirred for 1 h at room temperature. Clevios PH1000 (PEDOT:PSS) purchased from Heraeus Clevios GmbH was used as conducting polymer in this study. To control the weight ratio of PEDOT:PSS, PSSA (Mw: 75,000, Sigma-Aldrich) was directly added to the PEDOT:PSS solution at the weight ratio of 1:2.5 under magnetic stirring for 24 h. For the long-term stability test, neutral PEDOT:PSS solution was prepared by mixing acidic PEDOT:PSS solution with imidazole (Sigma-aldrich). The acidic and neutral PEDOT:PSS solutions show pH values of 1.8 and 7.0, respectively.

AgNW/PEDOT:PSS hybrid ink was fabricated by blending AgNW with PEDOT:PSS solution with different weight ratios. To increase the conductivity of PEDOT:PSS, 5 wt% dimethyl sulfoxide (DMSO) was added to PEDOT:PSS solution prior to blending with AgNW solution. In order to prepare the desired solutions with different AgNW/PEDOT:PSS weight ratios, the PEDOT:PSS mixture was slowly added to the AgNW solution according to the desired weight ratio.

### Fabrication of AgNW/PEDOT:PSS conducting films

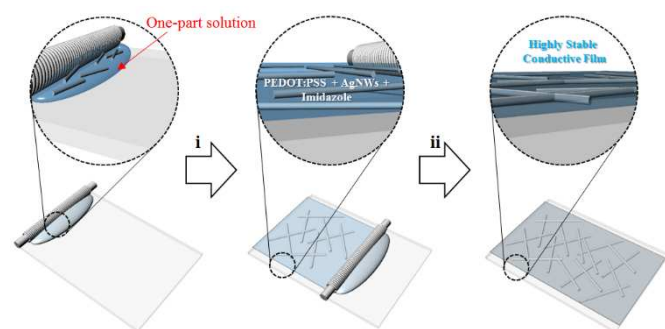
The AgNW/PEDOT:PSS ink was directly coated on A4-sized PET substrate by the Mayer rod coating technique. First, the fabricated AgNW/PEDOT:PSS ink was dropped on the top surface of the substrate and then the Mayer rod was quickly pulled down over the AgNW/PEDOT:PSS ink. Finally, the AgNW/PEDOT:PSS wet film spread over the surface of the substrate was dried at 150 °C for 2 min in a convection oven.

Large-scale AgNW/PEDOT:PSS conducting films were fabricated using the slot-die roll coating process at room temperature under ambient air condition. The AgNW/PEDOT:PSS ink was directly coated on the PET substrate without any filtration at the rate of  $2.7 \text{ m min}^{-1}$  with 460 mm in width. The film thickness was easily controlled by regulating the flow rate of the AgNW/PEDOT:PSS ink using the fluid-delivery system and the slot gap was fixed by a shim to 100  $\mu\text{m}$  in thickness. The coated AgNW/PEDOT:PSS wet

film was immediately dried at 150 °C for 3 min subsequent to the large-scale roll coating.

### Characterization of AgNW/PEDOT:PSS conducting films

The conductivities of PEDOT:PSS films spin-coated onto bare glass substrate ( $7.5 \times 7.5 \text{ cm}^2$ ) were measured by the van der



**Scheme. 1** Schematic illustration of the fabrication of highly conductive films with enhanced stability from PEDOT:PSS/AgNWs/Imidazole one-part solution. i) Bar coating and ii) drying process.

Pauw four-point technique (Keithley 2400 Source Meter). The sheet resistances were obtained using the four-point probe method (Napson, RT-70V/RG-5) by averaging the sheet-resistance values from 10 points for each sample. The transmittance values at 550 nm were obtained using a UV/Vis/NIR spectrophotometer (PerkinElmer, Lambda 750). The haziness value was measured also by a spectrophotometer (Nippon Denshoku, COH-400). All transmittance values were measured using a bare PET film as reference. The elemental composition of the AgNW/PEDOT:PSS film surface was analyzed by X-ray photoelectron spectroscopy (XPS, Thermo U. K., K-alpha) using monochromated Al K $\alpha$  X-ray radiation and by energy dispersive spectroscopy (EDS, JEOL, JSM-7001F). The morphological characterization was performed by means of field-emission scanning electron microscopy (FE-SEM, JEOL, JSM-6700F, JSM-7001F). Atomic force microscopy (AFM, Park System, XE-Bio) was used in non-contact mode to confirm the roughness of the film surfaces.

## Results and Discussion

AgNWs with average length of 20  $\mu\text{m}$  and average diameter of 57 nm (Fig. S1 in the Supporting Information) were used to fabricate the AgNW/PEDOT:PSS transparent conducting films, as shown in Scheme. 1. First, the electrical conductivities of the PEDOT:PSS films were determined prior to the study of the AgNW/PEDOT:PSS films in order to investigate the dependence of conductivity changes of PEDOT:PSS on the electrical properties of the resulting AgNW/PEDOT:PSS. The PEDOT:PSS films were prepared onto bare glass by spin-coating using various solutions with different weight ratios of PEDOT:PSS. Before spin-coating, PEDOT:PSS solutions were mixed with 5 wt% of dimethyl sulfoxide (DMSO), and then the solution mixtures were filtered through 0.45  $\mu\text{m}$  syringe filter (PVDF) to remove impurities and aggregated particles. As shown in Table. 1, the weight ratio of PEDOT in the

PEDOT:PSS solutions was controlled from 1:2.5 to 0.07:2.5 by adding PSSA to the PEDOT:PSS (1:2.5 weight ratio) solutions. PSSA generally dissociates into  $\text{H}^+$  and  $\text{PSS}^-$  in water,  $\text{PSSA} \rightarrow \text{H}^+ + \text{PSS}^-$ . As a result,  $\text{PSS}^-$  from PSSA acts as counter anion with positively charged PEDOT in PEDOT:PSS solution, similar to  $\text{PSS}^-$  from PEDOT:PSS. Fig. 1a shows the electrical

**Table. 1** The sheet resistance and transmittance of AgNW/PEDOT:PSS film as function of weigh ratio of PEDOT:PSS.

PEDOT <sup>a</sup>	PSS <sup>b</sup>	$R_s$ ( $\Omega \text{ sq}^{-1}$ )	T (%)
1.00	2.5	59.1	97.7
0.74	2.5	57.7	97.7
0.63	2.5	55.8	97.8
0.52	2.5	61.0	98.1
0.42	2.5	57.6	98.1
0.32	2.5	74.0	98.2
0.23	2.5	105.2	98.2
0.15	2.5	147.4	98.4
0.07	2.5	179.4	98.1

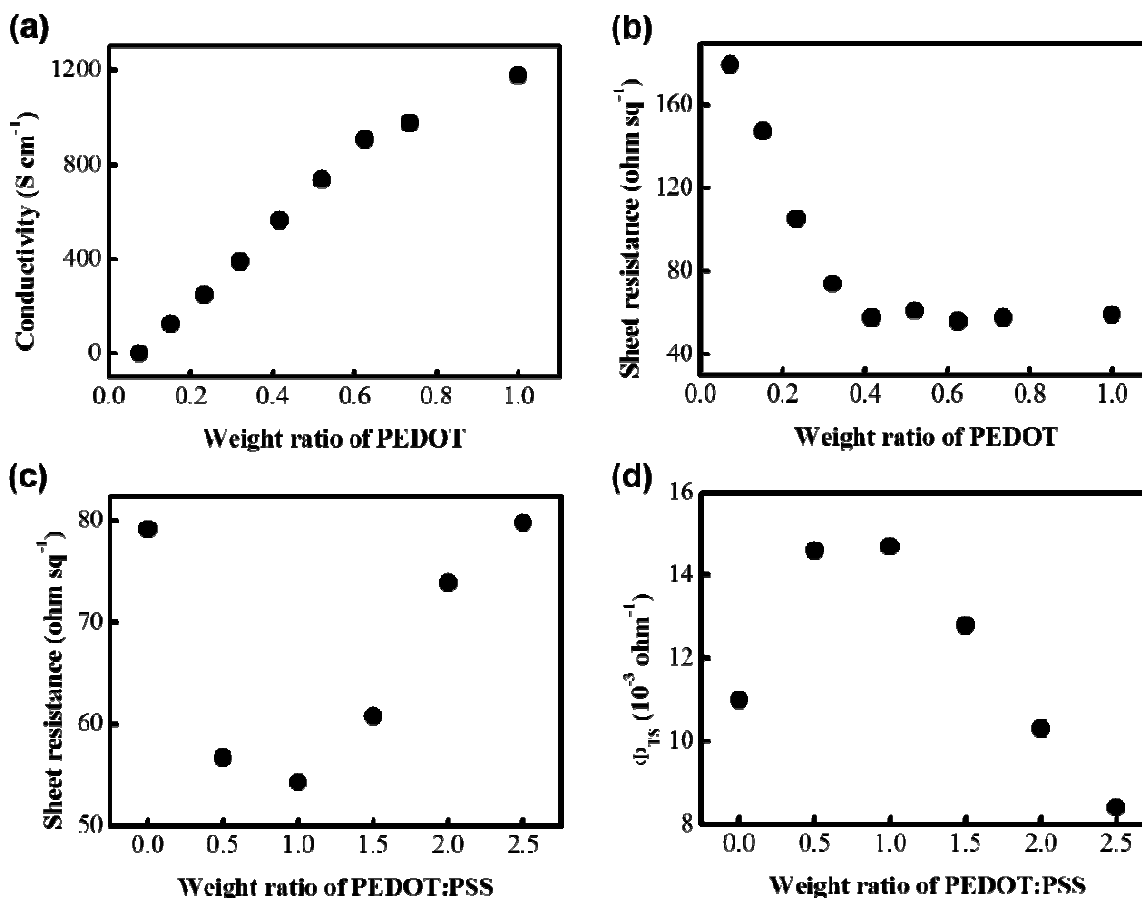
<sup>a</sup> Weigh ratio of PEDOT. <sup>b</sup> Weigh ratio of PSS.

conductivity of PEDOT:PSS films as a function of the PEDOT weight ratio in PEDOT:PSS solution. The electrical conductivity values linearly increased as the weight ratio of PEDOT increased because the electrical conductivity of PEDOT:PSS films is determined by the number of PEDOT domains. Therefore, minimization of  $\text{PSS}^-$  leads to maximization of PEDOT domains and reduction of the energy barriers for inter-chain and inter-domain charge hopping in the PEDOT:PSS films.<sup>22</sup> The AgNW/PEDOT:PSS conducting films were also coated on PET substrate of A4-paper size by the Mayer rod-coating technique, according to the weight ratio of PEDOT in PEDOT:PSS solution. The AgNW/PEDOT:PSS weight ratio (1:1) was fixed to investigate the influence of PEDOT:PSS on the electrical properties of the AgNW/PEDOT:PSS conducting films. As expected, the sheet resistance of the conducting films dramatically decreased from 179.4  $\Omega \text{ sq}^{-1}$  to 57.6  $\Omega \text{ sq}^{-1}$  with the increase in weight ratio of PEDOT from 0.07 to 0.42. The sheet resistance value saturated at the weight ratio of 0.42 (Fig. 1b). As reported in our previous study, the incorporation of PEDOT:PSS within AgNW networks can provide electrical pathways between non-connected AgNWs because PEDOT:PSS consists of highly conductive nanoparticles.<sup>23</sup> As a result, electrical charges can be more efficiently transported between AgNWs through PEDOT:PSS. However, the main electrical pathways are the AgNW channels in the conducting film due to the higher electrical conductivity of AgNWs compared to that of PEDOT:PSS.<sup>4</sup> Therefore, the sheet resistance of AgNW/PEDOT:PSS conducting films was determined by the current flowing through the AgNW channels and shows a different trend (saturated at 0.42 weight ratio of PEDOT:PSS) than the conductivity of PEDOT:PSS. This different behavior denotes that the conductivity of PEDOT:PSS of around  $\sim 600 \text{ S}$

$\text{cm}^{-1}$  is enough to improve the overall electrical conductivity of AgNW/PEDOT:PSS conducting films. To optimize the PEDOT:PSS weight ratio in the AgNW/PEDOT:PSS solution, conducting films with weight ratio of 0.42 of PEDOT in

PEDOT:PSS were also prepared using the same method and the electrical properties have been established according to the weight ratio of PEDOT:PSS in AgNW/PEDOT:PSS. As shown

Fig. 1 a) Conductivity and b) sheet resistance of PEDOT:PSS films according to the weight ratio of PEDOT in PEDOT:PSS solution. c) Sheet resistance and d) figure-of-merit values of AgNW/PEDOT:PSS films according to weight ratio of PEDOT:PSS in AgNW/PEDOT:PSS.



in Fig. 1c, the lowest sheet resistance was obtained at the weight ratio of 1.0 because the amount of PEDOT:PSS at this weight ratio is appropriate to completely fill the holes in the AgNW network, thereby optimally improving the film conductivity. In the case of a lower weight ratio, the holes were not completely filled with PEDOT:PSS and a large number of them remained in the AgNW/PEDOT:PSS conducting films. These remaining holes induce degradation of the electrical properties because the hole size is larger than the mean free path length of the charge carriers.<sup>20</sup> Therefore, electrical charges cannot be easily transported between non-connected AgNWs. In contrast, the main electrical pathways are changed from AgNWs to PEDOT:PSS at higher weight ratios of PEDOT:PSS to AgNW/PEDOT:PSS because the distance between AgNWs is significantly increased by reducing the AgNW density, in particular close to the percolation-threshold concentration. Thus, the sheet resistance of AgNW/PEDOT:PSS conducting films increases if the amount of PEDOT:PSS is in excess of AgNW. To determine the optimum ratio, the figure-of-merit  $\Phi_{TC}$  values according to the

different PEDOT:PSS weight ratios in AgNW/PEDOT:PSS were calculated by the Haacke equation.<sup>24</sup>

$$\Phi_{TC} = \frac{T^{10}}{R_s}$$

where  $T$  is the transmittance at 550 nm and  $R_s$  is the sheet resistance of the conducting film. The calculated  $\Phi_{TC}$  values are plotted in Fig. 1d. As expected, the maximum  $\Phi_{TC}$  value was obtained at the weight ratio of 1.0 ( $14.74 \times 10^{-3} \text{ ohm}^{-1}$ ). As mentioned above, the reason is that the minimum sheet resistance of the conducting film was obtained without loss in optical transmittance in case the PEDOT:PSS weight ratio in AgNW/PEDOT:PSS was 1.0. The detailed electrical and optical data according to the PEDOT:PSS weight ratio are presented in Table. S1.

The surface morphology of the AgNW/PEDOT:PSS conducting film with optimized weight ratio (PEDOT in PEDOT:PSS = 0.42, PEDOT:PSS in AgNW/PEDOT:PSS = 1.0) was characterized using scanning electron microscopy (SEM). As



shown in Fig. 2a, the fabricated conducting film is well structured without significant aggregations and overlapping regions of AgNWs, and the holes between the AgNWs are completely filled with PEDOT:PSS. The side-view image more clearly indicates that the AgNWs were densely embedded in the

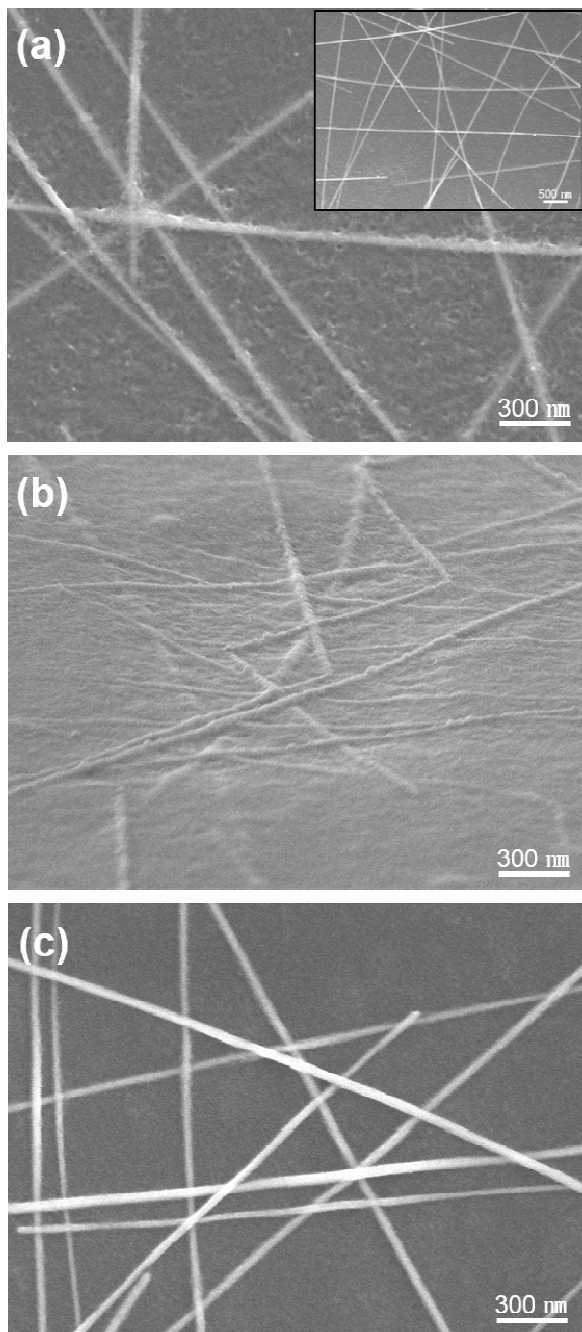


**Fig. 2** SEM images of a) top-view and b) side-view of the AgNW/PEDOT:PSS film with weight ratio of 0.42 (PEDOT in PEDOT:PSS) and 1.0 (PEDOT:PSS in AgNW/PEDOT:PSS). The inset shows the top-view image at larger magnification. c) Top-view SEM image of the bare AgNW film coated using the solution containing 0.5 wt% of dispersed AgNWs.

PEDOT:PSS matrix, as shown in Fig. 2b. This structure can significantly enhance the substrate adhesion because

PEDOT:PSS tightly binds AgNWs to the PET substrate.<sup>8</sup> In addition, the AgNW junctions can also be improved by the reduction of the contact resistance between AgNWs through the strong capillary forces occurring during film drying.<sup>25</sup> On the other hand, the bare AgNWs film exhibited a very rough surface (Fig. 2c). This rough surface made of protruding AgNWs leads to critical problems regarding its use as transparent electrode, induced by light scattering and electrical shorts.<sup>5,7,26–28</sup> Actually, the haziness value of bare AgNW film is two times higher than that of the AgNW/PEDOT:PSS film. However, the haziness was dramatically reduced by filling the AgNW network with PEDOT:PSS because the originally rough surface of the AgNW film becomes smoother. The measured haziness values of the AgNW and AgNW/PEDOT:PSS film were 4.18% and 1.91%, respectively.

The coexistence of AgNW and PEDOT:PSS within a single layer was further verified by X-ray photoelectron spectroscopy (XPS) and energy dispersive spectroscopy (EDS) (Fig. S2 and S3). As shown in Fig. S2c, the Ag 3d5/2 and 3d3/2 peaks of AgNW and S 2p peaks of sulfur atoms contained in PSS and PEDOT are clearly present at 368.1, 374.3, 168.4, 164.6, and 163.5 eV, respectively. In addition, the EDS spectrum of the AgNW/PEDOT:PSS conducting film strongly supports the fact that the conducting layer was composed of AgNW and PEDOT:PSS within a single layer (Fig. S3c). To clearly confirm the difference in surface topography and roughness between AgNW and AgNW/PEDOT:PSS films, atomic force microscopy (AFM) was performed for these two types of conducting films. Fig. 3 shows the AFM topographical images of the films. The root mean square (RMS) values of the bare AgNW and AgNW/PEDOT:PSS conducting films were 31.1 nm and 17.9 nm, respectively. As shown in Fig. 3a, the protruded AgNW clusters on the surface of the film are able to cause electrical shortcuts. The conducting film based on bare AgNWs undergoes degradation in device performance due to inefficient collection of free charge carriers arising from holes between AgNWs.<sup>4</sup> However, these problems can be easily overcome by the incorporation of PEDOT:PSS into the AgNW network, as shown in Fig. 3b. In particular, the AgNW/PEDOT:PSS conducting film showed much smoother surface compared to the bare AgNW film and, correspondingly, the roughness value was greatly reduced. This method provides a more effective fabrication process of conducting films with smooth surface without mechanical pressing and high-temperature annealing.

The performance of the AgNW/PEDOT:PSS conducting film was compared with previously reported results of AgNW/PEDOT:PSS transparent electrodes<sup>5–9</sup> by plotting the transmittance versus sheet resistance (Fig. 4). In general, the relationship between transmittance and sheet resistance of conducting films is given by:

$$T(\lambda) = \left(1 + \frac{188.5 \sigma_{OP}(\lambda)}{R_s \sigma_{DC}}\right)^{-2}$$

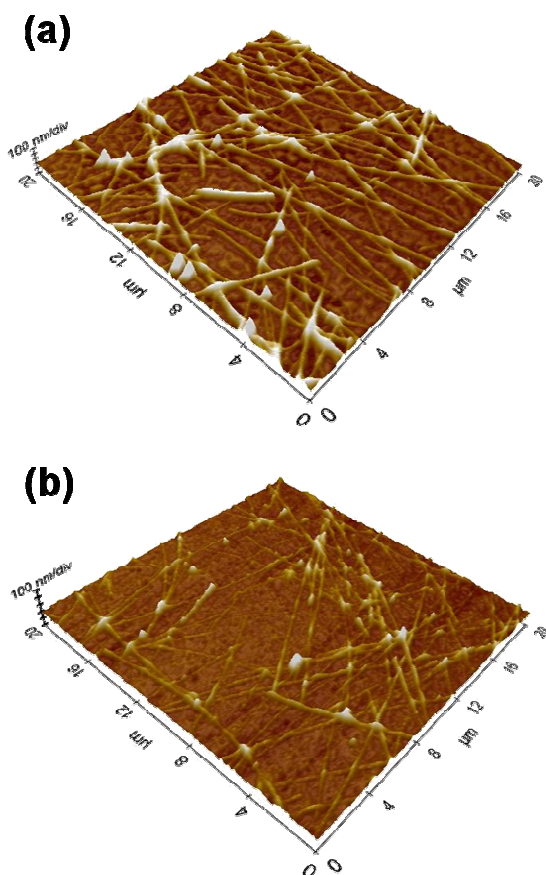


Fig. 3 AFM topological images of a) bare AgNW film coated using the solution containing 0.5 wt% of dispersed AgNWs and b) AgNW/PEDOT:PSS film with weight ratios of 0.42 (PEDOT:PSS) and 1.0 (AgNW/PEDOT:PSS).

Here,  $\sigma_{OP}(\lambda)$  is the optical conductivity and  $\sigma_{DC}$  is the DC conductivity of the film.<sup>29,30</sup> The value of  $\sigma_{DC}/\sigma_{OP}(\lambda)$  is widely used as another figure-of-merit to evaluate the performance of transparent electrodes. The four different curves corresponding to  $\sigma_{DC}/\sigma_{OP}(\lambda) = 100, 200, 300,$  and  $400$  are represented by dotted black lines. The  $\sigma_{DC}/\sigma_{OP}(\lambda)$  values of the presently investigated AgNW/PEDOT:PSS conducting film were in the range from 110 to 430. At the maximum  $\sigma_{DC}/\sigma_{OP}(\lambda)$  value of 429, the sheet resistance and transmittance were  $21.9 \Omega \text{ sq}^{-1}$  and 96.1%, respectively. This conductivity ratio is comparable to that of ITO film ( $\sigma_{DC}/\sigma_{OP}(\lambda) = 500$ ) and significantly higher than that of previously reported AgNW/conducting polymer films.<sup>5–10</sup> The reason for achieving the higher  $\sigma_{DC}/\sigma_{OP}(\lambda)$  value is that most of the AgNWs were more tightly embedded in the PEDOT:PSS matrix without defects between AgNW and PEDOT:PSS, compared to AgNWs over-coated with PEDOT:PSS. Due to the direct one-step coating using a single AgNW/PEDOT:PSS mixture, the fabricated conducting films showed much higher transmittance at the same sheet resistance. The other important factor is minimization of the bluish color of PEDOT:PSS by optimizing the PEDOT:PSS weight ratio. The bluish color of PEDOT:PSS film is mainly determined by the amount of PEDOT since PSS is highly transparent.<sup>31</sup>

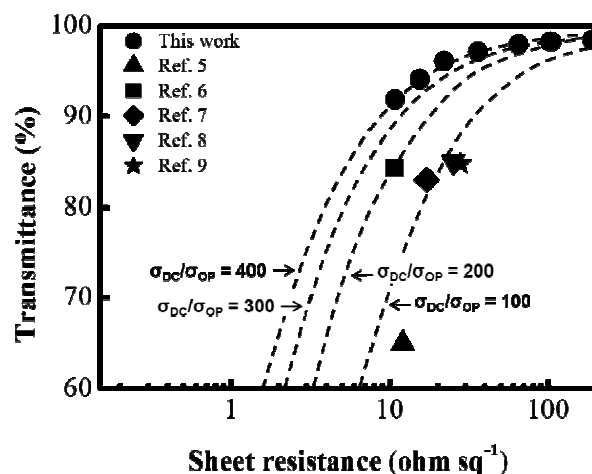


Fig. 4 Transmittance versus sheet resistance for the optimized AgNW/PEDOT:PSS film in comparison to previously published results

Therefore, highly transparent conducting electrodes could be obtained by using the optimized PEDOT:PSS ratio. Long-term stability tests were performed to investigate the relationship between the electrical properties of AgNW/PEDOT:PSS conducting films and the acidity of PEDOT:PSS. Normally, the strong acidity of PEDOT:PSS is well-known to induce poor stability of AgNWs by corrosion. Moreover, AgNWs exposed to ambient air are easily oxidized by atmospheric corrosion and form silver oxide ( $\text{AgO}$  or  $\text{Ag}_2\text{O}$ ) on the surface of AgNWs.<sup>6,9</sup> Fig. 5b and c show the sheet-resistance change of bare AgNW and AgNW/PEDOT:PSS conducting films under different external conditions. To confirm the influence of the acidity of PEDOT:PSS, two types of AgNW/PEDOT:PSS conducting films were prepared using acidic pristine PEDOT:PSS and neutralized PEDOT:PSS solution. Prior to the long-term stability tests, the conductivity of PEDOT:PSS was measured according to the pH value of PEDOT:PSS solution because the conductivity of PEDOT:PSS is dramatically degraded by shifting the pH from the acidic to the neutral range, due to dedoping of PEDOT:PSS.<sup>32,33</sup> PEDOT:PSS was neutralized using four kinds of base material to select the most suitable one. As shown in Fig. 5a, the conductivity of PEDOT:PSS mixed with either diethanolamine or triethanolamine is dramatically decreased by 20 and 27% at pH 3, respectively. On the other hand, the conductivity of PEDOT:PSS neutralized by either 2-dimethylaminoethanol or imidazole is gradually degraded by up to 14% and 17% at pH 7, respectively. These results show that mildly basic 2-dimethylaminoethanol and imidazole are more suitable for the neutralization of PEDOT:PSS without great conductivity loss. In this study, imidazole was chosen as main base material for neutralization because solid imidazole has higher melting and boiling point compared to 2-dimethylaminoethanol which is liquid at room temperature. Typically, azoles having nitrogen atoms in the backbone are widely used as copper corrosion inhibitor because the free electron pairs of the nitrogen atom can act as potential site for

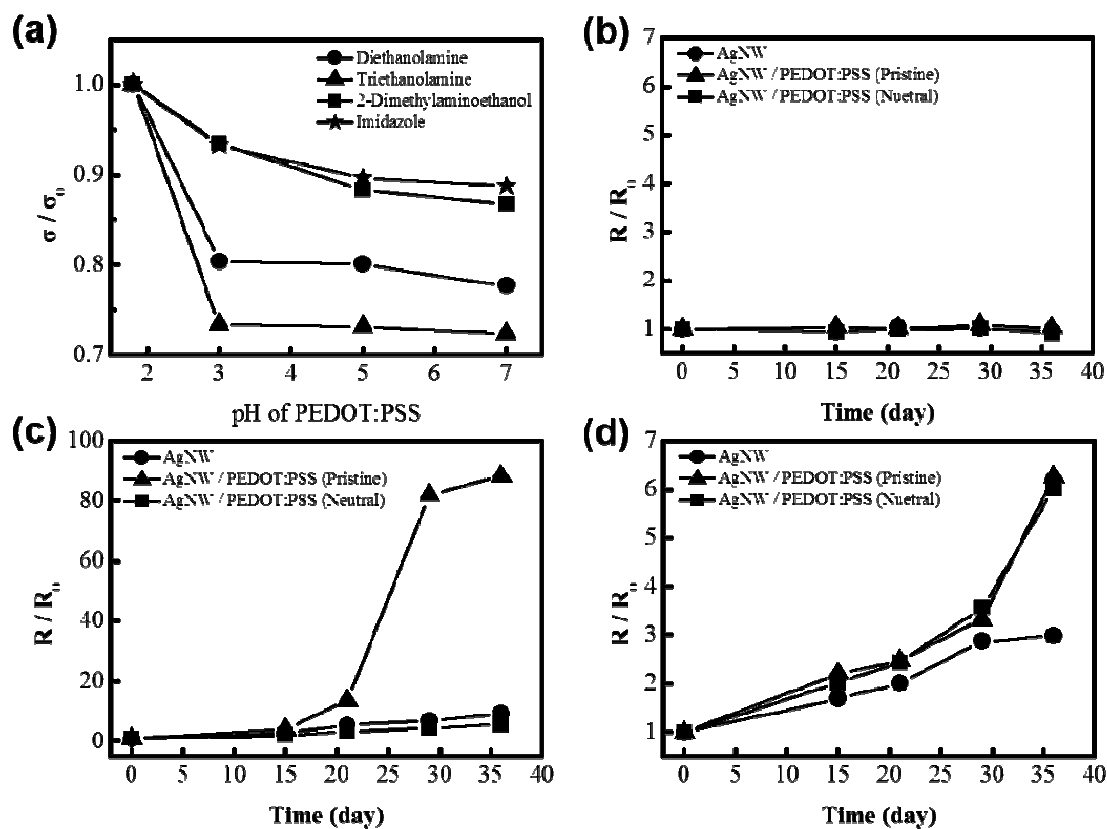


Fig. 5 a) Conductivity change of PEDOT:PSS as a function of the pH value controlled by different base materials. Normalized sheet resistance of bare AgNW, AgNW/acidic-PEDOT:PSS, and AgNW/neutral-PEDOT:PSS films in dependence of the exposure time at b) room temperature, c) high temperature (85 °C) and d) high temperature and high humidity (85 °C / 85%).

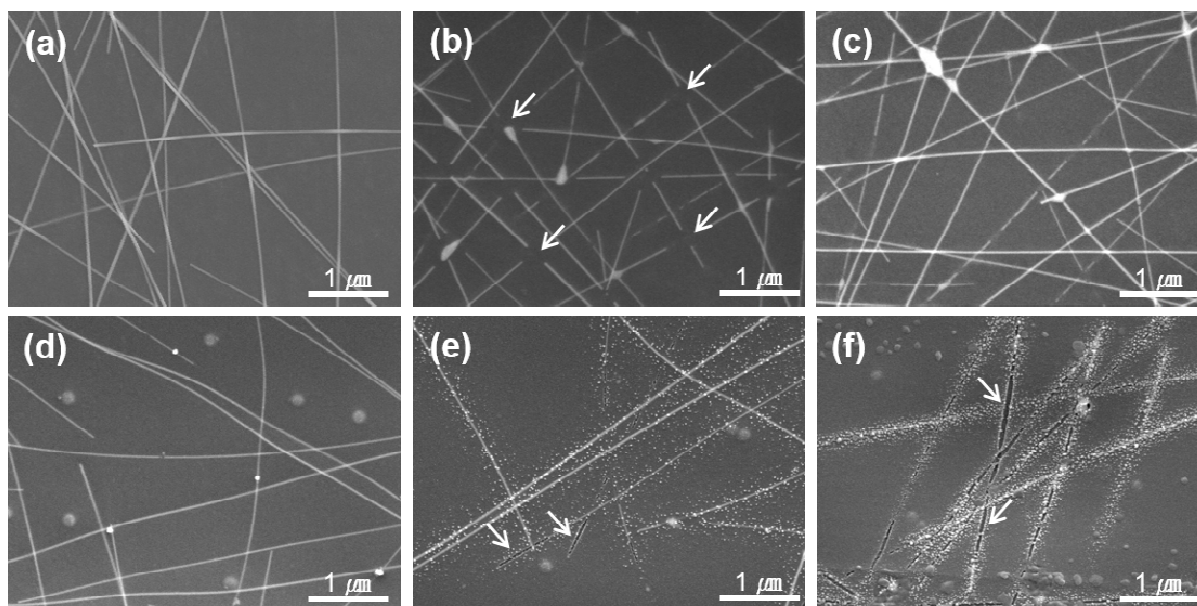


Fig. 6 SEM images presenting the surface morphology of the films after exposure for 36 days to (upper row) high temperature (85 °C) and (bottom row) high temperature and high humidity (85 °C / 85%) of a, d) bare AgNW, b, e) AgNW/acidic-PEDOT:PSS, and c, f) AgNW/neutral-PEDOT:PSS films. White arrows indicate defects induced by corrosion of AgNWs.



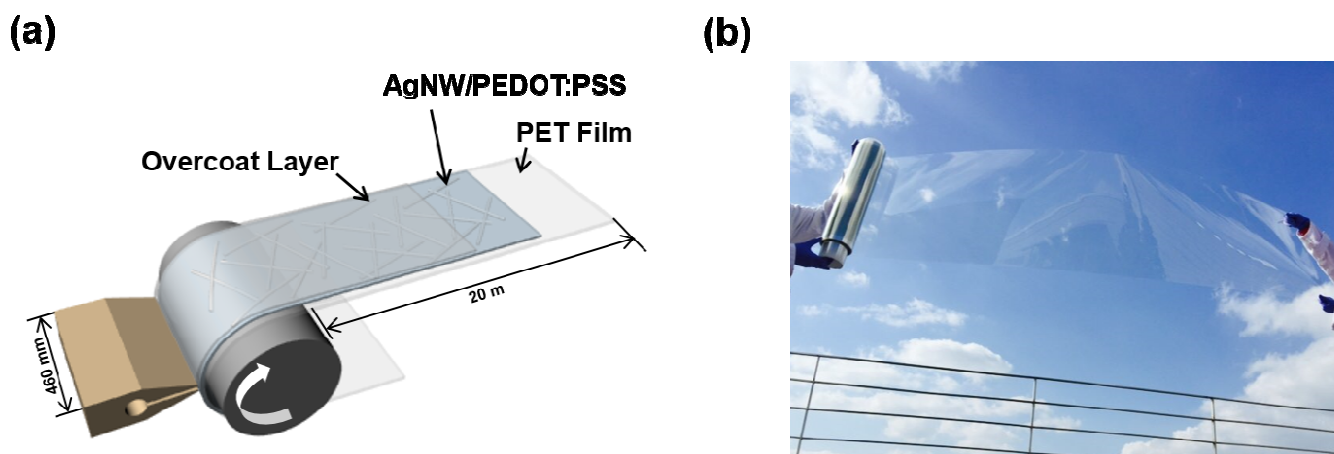


Fig. 7 a) Schematic diagram of slot-die roll-coating process and structure of the AgNW/PEDOT:PSS conducting film. b) Photographic image of the AgNW/PEDOT:PSS conducting roll film fabricated in this study.

bonding with copper and inhibiting action.<sup>34–36</sup> In the long-term stability tests, each prepared solution and film was exposed to room temperature, high temperature (85 °C), and high temperature / high humidity (85 °C / 85%) for 36 days. Fig. 5b shows the stability of bare AgNW and AgNW/PEDOT:PSS solutions. Each solution was packed in a 30 ml vial, exposed to room temperature during the stability test period, and freshly coated on PET substrate to obtain the sheet resistance value. All of the solutions did not show great changes in sheet resistance after 36 days because all solutions were isolated from external oxygen and the acidic corrosion of AgNWs caused by sulfonic acid was weak by the excessive dilution. In contrast, the sheet resistance of AgNW/acidic-PEDOT:PSS film exposed to high temperature increased more than eightyfold compared to its initial value. In addition, this value is over seventeen times higher than that of AgNW/neutral-PEDOT:PSS conducting film (Fig. 5c). However, when the films were exposed to high temperature and high humidity, the sheet resistances of both AgNW/acidic-PEDOT:PSS and AgNW/neutral-PEDOT:PSS films are similarly increased (Fig. 5d). Those results correspond to the SEM images shown in Fig. 6. Fig. 6a, b, and c show the surface morphologies of bare AgNW, AgNW/acidic-PEDOT:PSS, and AgNW/neutral-PEDOT:PSS conducting films, respectively, after exposure for 36 days at high temperature. Particularly, the AgNW/acidic-PEDOT:PSS film only showed a fragmentary morphology of discrete pieces against the bare AgNW and AgNW/neutral-PEDOT:PSS films, because the AgNWs were corroded by acidic PEDOT:PSS covered the surface of the AgNWs (Fig. 6b).<sup>11,12</sup> Usually, silver is insoluble in sulfonic acid at room temperature, though it can be dissolved in concentrated sulfonic acid under high-temperature condition. As a result, the sheet resistance of the AgNW/acidic-PEDOT:PSS film was significantly increased as the number of disconnected AgNWs increased. On the other hand, the bare AgNW and AgNW/neutral-PEDOT:PSS films maintained their electrical conductivity since their networks of AgNWs were not disconnected after 36 days at high temperature (Fig. 6a and c). Fig. 6d, e, and f show the surface morphologies of the films after exposure to high temperature and high humidity. In contrast to the results of the high-temperature test, the AgNWs of the AgNW/PEDOT:PSS films were surrounded by nanoparticles, regardless of the acidity of PEDOT:PSS. The reason why nanoparticles were formed is that atmospheric corrosion mainly occurred at the surface of AgNWs by the formation of hydrogen sulfide (H<sub>2</sub>S) and carbonyl sulfide (OCS) in the atmosphere.<sup>13–18</sup> The general reaction mechanism between silver and hydrogen sulfide is described by  $2\text{Ag} + \text{H}_2\text{S} \rightarrow \text{Ag}_2\text{S} + \text{H}_2$ . The silver sulfide formed on the surface of AgNWs is rather grown in form of nanoparticles, and the diameter of the AgNWs slowly decreases with the growth of these nanoparticles. Moreover, the moisture around the silver surface provides the silver sulfide with a dissoluble medium, and consequently silver corrosion is accelerated with increasing relative humidity. Moreover, the carbonyl sulfide rapidly decomposes to form hydrogen sulfide in the presence of water,  $\text{OCS} + \text{H}_2\text{O} \rightarrow \text{H}_2\text{S} + \text{CO}_2$ . The corrosion caused by sulfuration can be enhanced because carbonyl sulfide is the most abundant sulfur species in the atmosphere. In addition, since the sulfonic acid groups of PSS can easily absorb water, the structure of AgNWs filled with PEDOT:PSS has an adverse effect on the stability of AgNWs. As a result, the nanowire shape became gradually indistinct and finally transformed to silver sulfide nanoparticles after 36 days under high temperature and high humidity (Fig. 6e and f). Because atmospheric corrosion usually occurs regardless of the acidity of PEDOT:PSS, this problem can be overcome by protecting the AgNW/PEDOT:PSS conducting film from hydrogen sulfide and carbonyl sulfide in the atmosphere by using an overcoat layer.<sup>37–39</sup>

The mechanical flexibility of AgNW/PEDOT:PSS conducting film was also determined by monitoring the sheet resistance as a function of bending cycles. The bending test performed at the radius of curvature of 5 mm was progressed for up to 10000 bending cycles. As shown in Fig. S4, the sheet resistance only increased by 5.3% compared to its initial value. These results definitely

showed that this type of film is suitable to be applied as transparent conducting electrode in flexible electronics, such as flexible displays, touch screen panels, and wearable photovoltaics.

Large-scale AgNW/PEDOT:PSS conducting film was fabricated by direct coating on the PET substrate using the roll-to-roll slot-die coating method. A structure of the conducting film is illustrated in Fig. 7a. The sheet resistance of the conducting film was varied by the thickness control of the wet film by regulating the flow rate, as shown in Fig. S5a. After coating, a transparent overcoat layer based on tetraethyl orthosilicate (TEOS) was also deposited on the AgNW/PEDOT:PSS conducting film to protect the AgNWs from direct exposure to hydrogen sulfide and carbonyl sulfide. Finally, the AgNW/neutral-PEDOT:PSS coated, transparent, conducting, roll film (460 mm in width  $\times$  20 m in length) was successfully produced (Fig. 7b). This film exhibits suitable electrical ( $R_s \sim 75 \Omega \text{ sq}^{-1}$ ) and optical ( $T > 90\%$  at 550 nm, haziness  $\sim 1.21\%$ ,  $b^* \sim 0.72$ ) properties to replace the ITO film of touch screen panels (Fig. S5b). These optical properties were obtained using air as reference. Actually,  $R_s < 100 \Omega \text{ sq}^{-1}$ ,  $T > 90\%$ , haziness  $< 1.5\%$ , and  $b^* < 1.0$  of the transparent conducting film are required to make large-size capacitive touch screen panels.<sup>40</sup>

## Conclusions

We developed an effective method to fabricate highly conductive, transparent, and stable AgNW/PEDOT:PSS film without any post-treatment. The sheet resistance of the resulting conducting film was  $10.8 \Omega \text{ sq}^{-1}$  at the transmittance of 92%. Those excellent electrical and optical properties could be obtained by optimizing the weight ratio of PEDOT in PEDOT:PSS and PEDOT:PSS in AgNW/PEDOT:PSS. In addition, a much lower surface roughness of the conducting film appeared by filling the holes in the AgNW network with PEDOT:PSS. Corrosion of AgNWs caused by the acidity of PEDOT:PSS under high temperature condition was successfully prevented by neutralizing PEDOT:PSS using imidazole without serious conductivity loss. Because imidazole has high melting and boiling point compared to other base materials, it was chosen as the main base material for neutralization. In addition, azoles having nitrogen atoms in the backbone are widely used as copper corrosion inhibitor because the free electron pairs of the nitrogen atom can act as potential site for bonding with copper. Lastly, the AgNW/PEDOT:PSS coated, transparent, conducting, roll film (460 mm in width  $\times$  20 m in length) with good electrical ( $R_s \sim 75 \Omega \text{ sq}^{-1}$ ) and optical ( $T > 90\%$  at 550 nm, haziness  $\sim 1.21\%$ ,  $b^* \sim 0.72$ ) properties was produced using the roll-to-roll slot-die coating method. We believe that this approach will promote the development of large-scale metallic nanomaterial-based transparent electrodes with good flexibility, high efficiency, stability, and high quality, thus highly suitable for optoelectronic devices.

## Acknowledgements

This research was supported by the Nano•Material Technology Development Program through the National Research Foundation of Korea (NRF) funded by the Ministry of Science, ICT & Future Planning (MSIP, Korea) (NRF-2014M3A7B4050960, 2014M3A7B4051745 and 2014M3A7B4051749), the National Research Foundation of Korea (NRF) grant funded by the Korea government (MSIP) (No. 2007-0056091) and the Priority Research Center Program through the NRF funded by the the Ministry of Education, Science and Technology (No. 2009-0093823).

## Notes and references

<sup>a</sup> Department of Chemical and Biomolecular Engineering, Yonsei University, 50 Yonsei-ro, Seodaemun-gu, Seoul 120-749, Republic of Korea  
E-mail: jayhkim@yonsei.ac.kr

<sup>b</sup> Institute for Superconducting and Electronic Materials (ISEM), Australian Institute for Innovative Materials (AIIM), University of Wollongong, NSW 2500, Australia.

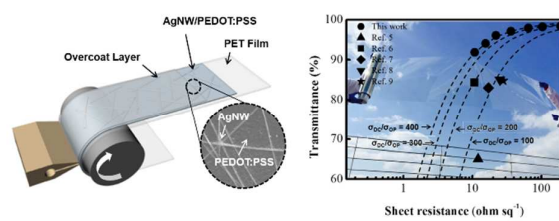
† Electronic Supplementary Information (ESI) available: [details of any supplementary information available should be included here]. See DOI: 10.1039/b000000x/

- 1 R. A. Hatton, M. R. Willis, M. A. Chesters, D. Briggs, *J. Mater. Chem.* 2003, **13**, 722
- 2 N. Formica, D. Sundar Chosh, T. L. Chen, C. Eickhoff, I. Bruder, V. Pruneri, *Sol. Energy Mater. Sol. Cells* 2012, **107**, 63
- 3 S. Ye, A. R. Rathmell, Z. Chen, I. E. Stewart, B. J. Wiley, *Adv. Mater.* 2014, **26**, 6670
- 4 A. Kim, Y. Won, K. Woo, S. Jeong, J. Moon, *Adv. Funct. Mater.* 2014, **24**, 2462
- 5 Y. J. Noh, S. S. Kim, T. W. Kim, S. I. Na, *Sol. Energy Mater. Sol. Cells* 2014, **120**, 226
- 6 D. Y. Choi, H. W. Kang, H. J. Sung, S. S. Kim, *Nanoscale* 2013, **5**, 977
- 7 W. Gaynor, G. F. Burkhard, M. D. McGehee, P. Peumans, *Adv. Mater.* 2011, **23**, 2905
- 8 J. Lee, P. Lee, H. B. Lee, S. Hong, I. Lee, J. Yeo, S. S. Lee, T. Kim, D. Lee, S. H. Ko, *Adv. Funct. Mater.* 2013, **23**, 4171
- 9 S. Chen, L. Song, Z. Tao, X. Shao, Y. Huang, Q. Cui, X. Guo, *Org. Electron.* 2014, **15**, 3654
- 10 A. B. V. K. Kumar, J. Jiang, C. W. Bae, D. M. Seo, L. Piao, S. Kim, *Mater. Res. Bull.* 2014, **57**, 52
- 11 Y. Ahn, Y. Jeong, Y. Lee, *ACS Appl. Mater. Interf.* 2012, **4**, 6410
- 12 H. Wu, L. Hu, M. W. Rowell, D. Kong, J. J. Cha, J. R. Mcdonough, J. Zhu, Y. Yang, M. D. McGehee, Y. Cui, *Nano Lett.* 2010, **10**, 4242

- 13 J. L. Elechiguerra, L. Larios-Lopez, C. Liu, D. Garcia-Gutierrez, A. Camacho-Bragado, M. J. Yacaman, *Chem. Mater.* 2005, **17**, 6042
- 14 H. E. Bennett, R. L. Peck, D. K. Burge, J. M. Bennett, *J. Appl. Phys.* 1969, **40**, 3351
- 15 J. P. Franey, G. W. Kammlott, T. E. Graedel, *Corros. Sci.* 1985, **25**, 133
- 16 T. E. Graedel, J. P. Franey, G. J. Gualtieri, G. W. Kammlott, D. L. Malm, *Corros. Sci.* 1985, **25**, 1163
- 17 L. Volpe, P. J. Peterson, *Corros. Sci.* 1989, **29**, 1179
- 18 T. E. Graedel, *J. Electrochem. Soc.* 1992, **139**, 1963
- 19 S. J. Lee, Y. Kim, J. K. Kim, H. Baik, J. H. Park, J. Lee, J. Nam, J. H. Park, T. Lee, G. Yi, J. H. Cho, *Nanoscale* 2014, **6**, 11828
- 20 L. Hu, H. S. Kim, J. Lee, P. Peumans, Y. Cui, *ACS Nano* 2010, **4**, 2955
- 21 A. R. Madaria, A. Kumar, F. N. Ishikawa, G. Zhou, *Nano Res.* 2010, **3**, 564
- 22 Y. Xia, K. Sun, J. Ouyang, *Adv. Mater.* 2012, **24**, 2436
- 23 S. Kim, S. Y. Kim, J. Kim, J. H. Kim, *J. Mater. Chem. C* 2014, **2**, 5636
- 24 G. Haacke, *J. Appl. Phys.* 1976, **47**, 4086
- 25 R. Zhu, C. Cheng, K. C. Cha, W. Yang, Y. B. Zheng, H. Zhou, T. Song, C. Chen, P. S. Weiss, G. Li, Y. Yang, *ACS Nano* 2011, **5**, 9877
- 26 L. Hu, D. S. Hecht, G. Gruner, *Chem. Rev.* 2010, **110**, 5790
- 27 J. S. Yeo, J. M. Yun, D. Y. Kim, S. Park, S. S. Kim, M. H. Yoon, T. W. Kim, S. I. Na, *ACS Appl. Mater. Interf.* 2012, **4**, 2551
- 28 D. S. Leem, A. Edwards, M. Faist, J. Nelsin, D. D. C. Bradley, J. C. de Mello, *Adv. Mater.* 2011, **23**, 4371
- 29 S. De, T. M. Higgins, P. E. Lyons, E. M. Doherty, P. N. Nirmalraj, W. J. Blau, J. J. Boland, J. N. Coleman, *ACS Nano* 2009, **3**, 1767
- 30 M. Dressel, G. Gruner, *Electrodynamics of Solids : Optical Properties of Electrons in Matter*, Cambridge University Press, Cambridge, UK 2002.
- 31 Y. H. Kim, C. Sachse, M. L. Machala, C. May, L. Muller-Meskamp, K. Leo, *Adv. Funct. Mater.* 2011, **21**, 1076
- 32 M. M. de Kok, M. Buechel, S. I. E. Vulto, P. van de Weijer, E. A. Meulenkaamp, S. H. P. M. de Winter, A. J. G. Mank, H. J. M. Vorstenbosch, C. H. L. Weijtens, V. van Elsbergen, *Phys. Stat. Sol. (a)* 2004, **201**, 1342
- 33 C. H. L. Weijtens, V. van Elsbergen, M. M. de Kok, S. H. P. M. de Winter, *Org. Electron.* 2005, **6**, 97
- 34 M. M. Antonijevic, M. B. Petrovic, *Int. J. Electrochem. Sci.* 2008, **3**, 1
- 35 M. Abdallah, I. Zaaferany, K. S. Khairou, M. Sobhi, *Int. J. Electrochem. Sci.* 2012, **7**, 1564
- 36 R. Gaasparac, C. R. Martin, E. Stupnisek-Lisac, *Int. J. Electrochem. Sci.* 2000, **147**, 548
- 37 Y. Jin, D. Deng, Y. Cheng, L. Kong, F. Xiao, *Nanoscale* 2014, **6**, 4812
- 38 P. Hsu, H. Wu, T. J. Carney, M. T. McDowell, Y. Yang, E. C. Garnett, M. Li, L. Hu, Y. Cui, *ACS Nano* 2012, **6**, 5150
- 39 I. K. Moon, J. I. Kim, H. Lee, K. Hur, W. C. Kim, H. Lee, *Sci. Rep.* 2013, **3**, 1112
- 40 D. S. Hecht, L. Hu, G. Irvin, *Adv. Mater.* 2011, **23**, 1482



## Table of contents



The AgNW/PEDOT:PSS coated, transparent, conducting, roll film (460 mm in width  $\times$  20 m in length) with good electrical and optical properties was produced using the roll-to-roll slot-die coating method.